(12) INTERNATIONAL APPLICATION PUBLISHED UNDER THE PATENT COOPERATION TREATY (PCT)

(19) World Intellectual Property Organization
International Bureau

(43) International Publication Date
31 January 2019 (31.01.2019)

WIPO | PCT

(10) International Publication Number
WO 2019/020201 A1

(51) International Patent Classification:
G01S 19/30 (2010.01) ***H04J 11/00*** (2006.01)
H04L 27/26 (2006.01) *G01S 19/02* (2010.01)
H04W 56/00 (2009.01)

(21) International Application Number:
PCT/EP2017/069235

(22) International Filing Date:
28 July 2017 (28.07.2017)

(25) Filing Language: English

(26) Publication Language: English

(71) Applicants: **EUROPEAN SPACE AGENCY** [FR/FR]; 8-10, rue Mario-Nikis, 75738 Paris Cedex 15 (FR). **AIRBUS DS GMBH** [DE/DE]; Robert-Koch-Strasse 1, 82024 Taufkirchen (DE).

(72) Inventors: **ÁVILA RODRÍGUEZ, José Ángel**; Keplerlaan 1, 2200 AG Noordwijk (NL). **ZANIER, Francesca**; Keplerlaan 1, Postnus 299, 2200 AG Noordwijk (NL). **FLOCH, Jean-Jacques**; Robert-Koch-Str. 1, D-82024 Taufkirchen (DE). **IOANNIDES, Rigas**; Keplerlaan 1, Postnus 299, 2200 AG Noordwijk (NL). **SOUALLE, Francis**; Robert-Koch-Strasse 1, 82024 Taufkirchen (DE). **WENDEL, Jan**; Robert-Koch-Strasse 1, 82024 Taufkirchen (DE).

(74) Agent: **DAVIES, Simon**; D Young & Co LLP, 120 Holborn, London EC1N 2DY (GB).

(81) Designated States *(unless otherwise indicated, for every kind of national protection available)*: AE, AG, AL, AM, AO, AT, AU, AZ, BA, BB, BG, BH, BN, BR, BW, BY, BZ, CA, CH, CL, CN, CO, CR, CU, CZ, DE, DJ, DK, DM, DO, DZ, EC, EE, EG, ES, FI, GB, GD, GE, GH, GM, GT, HN, HR, HU, ID, IL, IN, IR, IS, JO, JP, KE, KG, KH, KN, KP, KR, KW, KZ, LA, LC, LK, LR, LS, LU, LY, MA, MD, ME, MG, MK, MN, MW, MX, MY, MZ, NA, NG, NI, NO, NZ, OM, PA, PE, PG, PH, PL, PT, QA, RO, RS, RU, RW, SA, SC, SD, SE, SG, SK, SL, SM, ST, SV, SY, TH, TJ, TM, TN, TR, TT, TZ, UA, UG, US, UZ, VC, VN, ZA, ZM, ZW.

(84) Designated States *(unless otherwise indicated, for every kind of regional protection available)*: ARIPO (BW, GH, GM, KE, LR, LS, MW, MZ, NA, RW, SD, SL, ST, SZ, TZ, UG, ZM, ZW), Eurasian (AM, AZ, BY, KG, KZ, RU, TJ, TM), European (AL, AT, BE, BG, CH, CY, CZ, DE, DK, EE, ES, FI, FR, GB, GR, HR, HU, IE, IS, IT, LT, LU, LV, MC, MK, MT, NL, NO, PL, PT, RO, RS, SE, SI, SK, SM, TR), OAPI (BF, BJ, CF, CG, CI, CM, GA, GN, GQ, GW, KM, ML, MR, NE, SN, TD, TG).

(54) Title: A RECEIVER AND METHOD FOR PROCESSING A WIDE-BAND SIGNAL

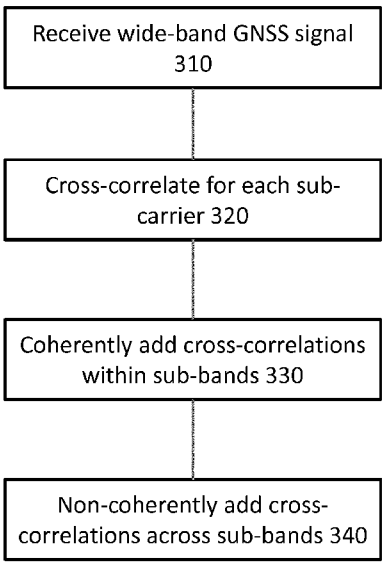


Figure 15

(57) Abstract: A method and receiver for processing a wide-band signal are provided. The receiver is configured to: receive a wide-band signal comprising N narrow-band signals, the wide-band signal using frequency division multiplexing to accommodate the N narrow-band signals on respective sub-carriers at different frequencies within the wide-band signal; divide the wide-band signal into P sub-bands, where P≥2, each sub-band comprising one or more sub-carriers, each sub-carrier accommodating a respective one of the N narrow-band signals, and at least one sub-band comprising two or more sub-carriers; for each of the N narrow-band signals, correlate the received narrow-band signal to produce a sub-carrier cross-correlation function; for each sub-band, coherently sum the one or more sub-carrier cross-correlation functions for that sub-band to create a sub-band cross-correlation function; and sum non-coherently the sub-band cross-correlation functions of all of the P sub-bands to produce a cross-correlation function for the wide-band signal. In some implementations, the wide-band signal comprises a wide-band global navigation satellite system (GNSS) signal comprising a spreading code, and the receiver is configured to use the received spreading code for determining the location of the receiver.

WO 2019/020201 A1

[Continued on next page]

Published:
— *with international search report (Art. 21(3))*

A RECEIVER AND METHOD FOR PROCESSING A WIDE-BAND SIGNAL

Field

The present invention relates to a receiver and method for processing a wide-band signal, for example, for use in conjunction with a satellite navigation system.

Background

Global navigation satellite systems (GNSS) are becoming increasingly important in a wide range of applications, including handheld devices for position determination, in-car navigation support, and so on. A satellite navigation system comprises a constellation of satellites, each of which broadcasts one or more signals to earth. The basic components of a satellite signal are a spreading code (also referred to as a positioning, synchronisation or ranging code) which is combined with navigation data. The resulting combination is then modulated onto a carrier at a set frequency for (repeated) transmission to earth. Each satellite generally transmits at multiple frequencies, which can help to compensate for ionospheric effects, to improve accuracy, to offer different services, etc.

The spreading code component of a satellite signal typically comprises a predetermined sequence of bits (referred to as 'chips') and is used to perform two main tasks. Firstly, the spreading code provides a synchronisation and access (CDMA) mechanism to allow a receiver to lock onto a satellite signal. Thus each satellite (and typically each signal broadcast from that satellite) has its own synchronisation code. When a receiver is first switched on, it may not know which satellite signals can be received, since certain satellites in the constellation will be below the horizon for that particular location at that particular time. The receiver uses the synchronisation codes to lock onto a signal from a first satellite. Once this has been done, the navigation data in the signal can be accessed. This then provides almanac data for the other satellites in the constellation, and allows the remaining satellites that are visible to the receiver to be acquired relatively quickly. Some receivers may be able to retrieve almanac data from alternative sources, e.g. over the Internet.

The spreading code provides a distance estimate from the satellite to the receiver, based on the time taken for the signal to travel from the satellite to the receiver. The position of the receiver is then determined in three-dimensional space by using a process of

trilateration, given the known positions of the satellites (as specified in the navigation data received from the satellites). In theory, trilateration can be performed with signal information from a minimum of three satellites, assuming that the timing offset between the receiver clock and satellite clocks is known. In practice, this timing offset is generally unknown, except for specialised receivers, so that signal information is obtained from at least one additional satellite to compensate for the unknown time offset at the receiver. If signals from further satellites are available, a statistical position determination can be performed using any appropriate algorithm such as least squares. This can also provide some indication of the error associated with an estimated position.

One important parameter for a spreading code is the chip rate at which the spreading code is transmitted, since this in turn controls the accuracy with which the positional determination can be made. Another important parameter for a spreading code is its total length, in other words the number of chips in the spreading code before it repeats. One reason for this is that the finite length of a spreading code can lead to ambiguity in the position determination. A longer length for the spreading code reduces such ambiguity, and also provides better separation of signals from different sources and increased robustness against interference. On the other hand, having a longer repetition length for the spreading code may delay initial acquisition of the signal, as well as requiring more processing capability within the receiver. In general, the length of the spreading code also impacts the data rate that can be used for the navigation data, since there is normally only one bit of navigation data for each complete spreading code sequence. Therefore, the longer the repetition length for the spreading code, the lower the bit rate for the navigation data.

Spreading codes for use in a GNSS are typically generated or created to have specific intra-code and inter-code correlation properties. The inter-code correlation properties relate to the cross-correlation function (CCF) between different codes from different satellites – these should be small (ideally zero) for all relative offsets between the codes, in order to allow the signal from each individual satellite to be uniquely identified. The cross-correlation properties are therefore important for signal acquisition, since they help to prevent a synchronisation code from one satellite being accidentally mistaken for a synchronisation code from another satellite. The intra-code correlation properties relate to the auto-correlation function (ACF) of a single code from a single satellite. The ACF will (necessarily) have a peak at zero timing offset. However, the ACF for a spreading code should also be small (ideally zero) for all other (non-zero) offsets, to ensure the receiver

properly locks onto the peak for zero time offset (rather than another ACF peak at non-zero offset).

Many receivers employ a two-phase acquisition process. In the first phase, the receiver performs a correlation of the incoming signal against the set of satellite spreading codes. In particular, the receiver searches for a spreading code from any satellite, allowing for any timing offset between the satellite and the receiver, and for any Doppler frequency shift between the satellite and the receiver (which is dependent on the motion of the satellite in space relative to the user). If a correlation value is found to exceed a predetermined threshold, then a second phase involving a more detailed analysis is performed for the relevant combination of satellite spreading code, timing offset and Doppler shift. This second-phase analysis verifies and confirms or if necessary rejects the initial coarse acquisition.

Additional information about satellite navigation systems can be found in: "Global Positioning System: Signals, Measurements and Performance", by Misra and Enge, Ganga-Jamuna Press, 2001, ISBN 0-9709544-0-9; "Global Positioning System: Theory and Applications", Vol 1 and Vol 2, by Bradford W. Parkinson and James J. Spilker Jr, ISBN 1-56347-106-X, published by the American Institute for Aeronautics and Astronautics; "Galileo User Segment Overview" by Hollreiser et al, ION GPS/GNSS 2003, September 2003, Portland, Oregon, p1914-1928; and "Galileo Test User Segment - First Achievements and Application", by Hollreiser et al, GPS World, July 2005. Example implementations of a GNSS are described in WO 2006/063613 and WO 2007/101454.

A particular focus for a GNSS is to provide a very precise location of the receiver. This depends on determining the travel time (code delay) of the received spreading code as accurately as possible, which in turn depends on identifying the location of the ACF peak as accurately as possible. Most spreading codes are chosen to have an ACF of zero for an offset of ± 1 (in units of the chip duration). This then gives a known, triangular shape for the ACF peak. In practice, the location of the ACF peak (and hence the travel time of the received signal) can then be estimated to some fraction of a chip duration, allowing for factors such as noise and any slight mismatch of the received spreading code frequency with that utilised by the receiver.

In order to reduce the timing uncertainty associated with the ACF peak, and hence improve the estimated location accuracy, the chip duration could be shortened. However, as

discussed above, there are already some constraints on the overall duration of the spreading code, as well as the number of chips in the spreading code, so reducing chip duration impacts other operational aspects of a GNSS. An alternative approach, which has been adopted for the Galileo GNSS, is to use binary offset carrier (BOC) signals for the modulation of the transmitted navigation signals (instead of standard binary phase shift keying (BPSK) modulation). This involves multiplying the spreading code by a higher frequency subcarrier, i.e. there are typically multiple bits of the subcarrier for each chip duration.

The effect of BOC modulation is to replace the original ACF peak (as obtained from BSPK modulation) with a narrower, but split, ACF peak. The narrower ACF peak permits improved better code tracking accuracy and improved location estimates (compared to the BPSK modulation). However, this is at the cost of introducing, as a result of the splitting, additional correlation peaks into the ACF, which leads to a potential ambiguity in the estimated code delay. There is a risk that a receiver may incorrectly lock onto one of these additional peaks, rather than the narrower original (central) ACF peak, thereby causing an error or bias in the code delay estimation (and hence a position error). EP3104195 describes a method for tracking such a BOC signal to help overcome this risk.

More generally, reducing the timing uncertainty associated with the received spreading code normally implies the provision of higher frequency components in the spreading code signal (whether by modulation or by reducing the chip duration) in order to allow a better time definition of the spreading code signal. These higher frequency components then require a wider modulation band in order to be accommodated within the carrier signal (sometimes referred to as a wide-band signal).

Although the use of a wide-band signal for a GNSS can help to enhance positioning accuracy, conversely it can cause a problem for signal acquisition. Thus as mentioned above, the receiver typically has to search through Doppler frequency space to acquire a satellite by finding a correlation peak. Any slight offset between the search frequency and the received frequency will result in a loss of phase over the duration of the correlation, thereby reducing the correlation peak, and eventually eliminating the correlation peak at a large enough (limiting) offset. The granularity of the Doppler frequency search must therefore be suitably smaller than this limiting frequency offset in order to ensure that a correlation peak is not missed. The loss of phase occurs more quickly for a signal with higher frequency components, so that a wide-band GNSS signal has a smaller limiting offset. This implies that

such a signal requires a smaller granularity for the Doppler frequency search, i.e. the interval between trial frequencies in the search space must be reduced, which in turn increases the number of trial frequencies to be tested. Consequently, for a receiver with a fixed number of correlators (which determines the number of trial frequencies that can be tested in parallel), the use of a wide-band GNSS with more trial frequencies to be tested will generally delay signal acquisition compared to a narrow-band GNSS.

Summary

The invention is defined in the appended claims.

A method and receiver for processing a wide-band signal are provided. The receiver is configured to: receive a wide-band signal comprising N narrow-band signals, the wide-band signal using frequency division multiplexing to accommodate the N narrow-band signals on respective sub-carriers at different frequencies within the wide-band signal; divide the wide-band signal into P sub-bands, where $P \geq 2$, each sub-band comprising one or more sub-carriers, each sub-carrier accommodating a respective one of the N narrow-band signals, and at least one sub-band comprising two or more sub-carriers; for each of the N narrow-band signals, correlate the received narrow-band signal to produce a respective sub-carrier cross-correlation function; for each sub-band, coherently sum the one or more sub-carrier cross-correlation functions for that sub-band to create a sub-band cross-correlation function; and sum non-coherently the sub-band cross-correlation functions of all of the P sub-bands to produce a cross-correlation function for the wide-band signal.

Such a method may be used for acquisition of the received signal and/or for accessing data encoded in the received signal. In some implementations, the wide-band signal comprises a wide-band global navigation satellite system (GNSS) signal comprising a spreading code, and the receiver is configured to use the received spreading code for determining the location of the receiver.

Brief Description of the Drawings

Various embodiments of the invention will now be described in detail by way of example only with reference to the following drawings:

Figure 1 is a graph of the power spectral density of an example multi-carrier signal as used in the approach described herein.

Figure 2 is a graph of the correlation function for the wide-band acquisition of the example multi-carrier signal of Figure 1.

Figure 3 shows a detail of the central three peaks of Figure 2 using a logarithmic scale and marks the 3dB fall-off.

Figure 4 is a graph of the correlation function for the narrow-band acquisition of the example multi-carrier signal of Figure 1, again showing the 3dB fall-off.

Figure 5 is a graph of the correlation function for the sub-band acquisition of the example multi-carrier signal of Figure 1, using 4 sub-bands, in accordance with the approach described herein, and again showing the 3dB fall-off.

Figure 6 is a graph plotting acquisition dwell time against carrier-to-noise ratio for wide-band acquisition (light line) and sub-band acquisition (dark line) of the example multi-carrier signal of Figure 1.

Figure 7 is a diagram of an example modulation scheme for a multi-carrier signal as used in the approach described herein, showing the allocation of symbols to sub-carriers.

Figures 8-13 are variations on the modulation scheme of Figure 7, in which the allocation of symbols to sub-carriers is subject to one or more constraints.

Figure 14 is a simplified schematic diagram of a portion of an example receiver implementing the approach described herein.

Figure 15 is a schematic flowchart of an example method implemented by a receiver using the approach described herein.

Detailed Description

There are various ways to improve signal robustness at a receiver, such as increasing the transmission power from the transmitter (e.g. satellite), utilising more bandwidth for the signal, using an enhanced format for the signal (increased signal intelligence), and/or applying complex receiver techniques and/or hardware. The approach described herein is based on using a wider signal bandwidth in conjunction with more intelligent signal design/processing (in contrast to using additional power at the satellite level, which is an expensive resource, or adding significant complexity to the receivers, which are ideally low-cost devices).

The approach described herein helps receivers having low to medium cost and complexity exploit wide-bandwidth signals that would otherwise require a relatively high level of hardware resources, and so makes the services associated with such signals accessible to and attractive for a larger number of users. In addition, service providers can expand their services to include more user applications that might not otherwise be viable if restricted to high-cost receivers.

The approach described herein can be used to help receivers acquire a wide-band signal. The approach is flexible across different grades of receiver, thereby supporting the use of modern wide-band signal modulation, and can be tailored to application performance requirements and receiver hardware cost and complexity. Furthermore, the present approach is a parametric solution, in that different receivers can be configured differently, e.g. based on their available hardware resources. In addition, individual receivers may be configured differently at different times, for example based on application requirements, as well as expected (or current) operational conditions.

The approach described herein is particularly suited to use in satellite communication and navigation systems that provide wide-band signals including multiple (sub)carriers, like OFDM-CDMA (orthogonal frequency division multiplex, code division multiple access). This type of modulation offers various benefits, including robustness against interference, higher effective data rate and more accurate synchronization of receivers. In addition, the receiver synchronization function (i.e. locking onto the correct auto-correlation peak), which is the primary objective for a GNSS service, is improved with such increased satellite signal bandwidth.

On the other hand, a wide-band signal leads to a narrower correlation function. Although this may offer advantages in signal tracking, plus handling multipath and a noisy environment, the processing and tracking of such wide-band signals comes with a penalty in receiver cost and complexity. In particular, wide-band signal processing strategies generally require a narrower correlator spacing for a code discriminator to track the signal - which in turn requires a higher sampling rate (in frequency space) and an increased number of correlators. This in turn imposes a higher demand upon receiver hardware resources and power consumption.

The situation for acquisition tends to be even more complex, since for a wide-band signal, the main peak of the correlation function is very narrow, so that the number of

hypotheses for the code search is extremely high. Therefore, either the receiver architecture must become more complex with a high number of correlators, or the acquisition will take longer (and may potentially fail, e.g. due to receiver movement).

One way to interpret the OFDM signal is as a sum of elementary narrow-band signals, all offset with respect to a central carrier frequency, and to process them non-coherently for acquisition: each narrow-band signal is for example down-converted to the carrier and correlated with a replica matched to the corresponding narrow-band signal. Such a solution is able to generate a cross-correlation function which is wider (than for the original wide-band signal), thereby enabling a relaxation (reduction) in the number of code hypotheses to be searched. However, the draw-back of such a solution is that the non-coherent summation of the cross-correlation functions for the individual narrow-band signals leads to relatively large, and potentially unacceptable, squaring losses, especially as the number of OFDM components increases.

The present approach can be considered as an intermediate strategy, between wide and narrow-band processing, which can be used to reduce the number of hypotheses while incurring only limited squaring losses due to non-coherent summation of the correlation functions. In this approach, selected subcarrier signals are correlated coherently within sub-bands, and the sub-bands are then combined non-coherently. In particular, the wide-band signal is divided into sub-bands, each sub-band containing at least one narrow-band signal (from a respective sub-carrier). The selection of the group of sub-carrier signals within each sub-band generally takes into consideration ionosphere group delay, so that the coherent summation within a sub-band is not sensitive to such ionospheric effects. Accordingly, the cross-correlation functions for each of the narrow-band signals within a sub-band are added coherently, while the resultant sub-band cross-correlation functions are added non-coherently. Since the allocation of sub-carriers to sub-bands is flexible, the approach described herein allows the complexity of the correlation calculations to be configured or changed, dependent on the receiver grade and application requirements, as well as expected user operational conditions.

For example, a receiver manufacturer may define a range of receivers from high-end to low-end. The former may have increased hardware complexity, including many correlators to support searching a large number of frequencies at maximum sensitivity. Conversely, the latter might have fewer correlators, so that a smaller number of frequencies

are searched; this can be supported with only a small loss in sensitivity by using a limited number of non-coherent summations of correlations.

The approach described herein is well-suited to satellite communication and navigation systems, which have an increasing focus on the use of wide bandwidth modulations to increase the data rate, robustness and accuracy of the provided services. Although current satellite technology is able to generate such modulations, at the receiver end the technology to acquire such signals is relatively high cost and complex. The present approach helps different receiver grades to acquire and thus make use of such modulations. The present approach may also be utilised for non-space activities, including terrestrial communication signals (4G/5G) that use multi-carrier modulations and radar applications that are based on frequency modulated signals. Scientific applications based on the scanning of frequency dispersive properties of a medium, for example, as in ionospheric monitoring, may also benefit from this approach.

The following equation provides a generic expression of a data modulated multicarrier signal (like Orthogonal Frequency Division Multiplexing) composed of N_{sc} frequencies:

$$s(t) = \sum_{i=1}^{N_{sc}} d_i(t) \times \exp(2\pi j f_i t) \times p(t) \times c(t) \quad \text{- (Equation 1)}$$

In Equation 1:

- N_{sc} represents the number of sub-carrier frequencies
- f_i represents each sub-carrier frequency
- p(t) is a pulse shape which modulates each sub-carrier frequency
- c(t) is a spreading code sequence which modulates each sub-carrier frequency for a given satellite
- $d_i(t)$ is a data symbol applied to each sub-carrier frequency

For a GNSS transmission, $d_i(t)$ corresponds to the navigation data. In general, one bit of navigation data is transmitted for each repetition of the spreading code sequence (in effect, the value of the bit of navigation data determines whether the spreading code sequence is

transmitted with odd or even polarity). The spreading code sequence c(t) is known at the receiver (or at least the set of spreading code sequences for the GNSS is known), but not the value of the navigation data $d_i(t)$. For normal data communications, e.g. OFDM communications, $d_i(t)$ represents as data bit to be transmitted, and there is no spreading code, i.e. in effect, we can set c(t) =1.

Usually N_{sc} equals 2^L in order to facilitate the modulation and demodulation of the corresponding symbols. Hence at each time epoch, t, at most N_{sc} symbols are modulated simultaneously. We can consider as each sub-carrier as supporting or representing a narrow-band signal, and the full set of N_{sc} sub-carriers as supporting or representing, in combination, a wide-band signal.

An elementary cross-correlation function (CCF) is defined as follows between the received version of the signal s(t) and a sub-carrier of index i. In effect, this cross-correlation function of Equation 2, provides an estimate of the (demodulated) data symbol $d_i(t_k)$, i.e. the data symbol applied to sub-carrier *i* of the received signal *s(t)* at time epoch t_k, based on the assumed values for τ' and $f_{d'}$ (as defined below):

$$CCF_i\ (\Delta\tau, \Delta f_d, t_k) = \int_{t_{k-1}}^{t_k} s(t) \times (\exp(2\pi j(f_i + \Delta f_d) \times (t - \Delta\tau)) \times p'(t - \Delta\tau))dt$$

(Equation 2)

In Equation 2:

- $\Delta\tau$ is τ'-τ and represents the code delay misalignment error
- Δf_d is $f_{d'}$-f_d and represents the Doppler frequency misalignment error
- τ is the code delay between the satellite and the receiver
- f_d is the Doppler frequency
- τ' is the code delay hypothesis between the satellite and the receiver
- $f_{d'}$ is the Doppler frequency hypothesis
- p'(t) = p(t) × c(t) (for conciseness)

Note that the timing interval from t_{k-1} to t_k will generally correspond to the duration of one bit of (e.g. navigation) data, $d_i(t_k)$, which also represents the time for a complete spreading code sequence c(t) to be transmitted. In addition, it will be appreciated that for GNSS acquisition, there may also be a need to test for multiple different satellites (if it is not known which satellites are visible). This then provides an extra dimension for the acquisition procedure, namely testing with different sequences for c(t) to identify respective satellite signals. In Equation 2, if the assumed spreading code sequence c(t) does not match the spreading code sequence used to generate s(t), then this mismatch will result, in effect, in the output of Equation 2 being zero – i.e. no signal detected. In contrast, if the assumed spreading code sequence c(t) does match the spreading code sequence used to generate s(t), and assuming that appropriate values are adopted for the Doppler and code delay hypotheses, the (normalised) output of Equation 2 will be ±1, reflecting the value of $d_i(t_k)$.

For the following discussion (but without limitation), we assume that one bit of data $d(t_k)$, e.g. navigation data, is transmitted for time interval from t_{k-1} to t_k. This single bit of data then determines the values of $d_i(t_k)$ for this time interval according to a known mapping or arrangement. For example, a simple arrangement would be that $d_i(t_k) = d(t_k)$ for all values of i, i.e. the same value of $d(t_k)$ is transmitted on each of the N_{sc} sub-channels. (Alternative arrangements are discussed below).

During the acquisition process the receiver tests multiple code delay ($\Delta\tau$) and Doppler frequency (Δf_d) hypotheses. The hardware complexity (number of correlators for active acquisition, Tap delay lines for the passive matched filter acquisition, FFT for massive parallel search, etc …) directly depends on the mesh of the grid of hypotheses, so it is necessary to adopt an appropriate discretisation of the code delay-Doppler uncertainty space.

The cross-correlation function applicable for wide band acquisition can be calculated using Equation 3 below, assuming that the N_{sc} modulation symbols transmitted at time t_k are known at the receiver side (n_i^{Rx})

$$\left|CCF_{WB}\left(\Delta\tau,\Delta f_d,t_k\right)\right| = \sqrt{\left|\sum_{i=1}^{N_{sc}} d_i^{Rx}(t_k)\times\left(CCF_i\ \left(\Delta\tau,\Delta f_d,t_k\right)\right)\right|^2} \quad \text{- (Equation 3)}$$

In Equation 3, $d_i^{Rx}(t_k)$ represents the modulation signal at time t_k. In particular, we assume that $d(t_k)=1$, and then generate the values of $d_i^{Rx}(t_k)$ using the known mapping as

discussed above. Therefore $d_i^{Rx}(t_k)$ represents a signal to test against the output from Equation 2. In other words, Equation 3 can be considered as a cross-correlation between the received symbol (as determined from signal *s(t)*) and assumed test signal ($d_i^{Rx}(t_k)$), summed over the full set of N_{sc} sub-carriers.

As explained above, if this full wide-band correlation is performed, the correlation function will be very narrow, in the sense of being very sensitive to any slight error or misalignment of the code delay ($\Delta\tau$) and Doppler (Δf_d) hypotheses. Consequently, the hypothesis grid must be made much finer (more closely spaced) in Doppler frequency and code delay space in order to ensure any correlation peak is properly detected.

In Equation 3, all of the N_{sc} sub-carriers are summed coherently. Coherent summation implies summation of the cross-correlation function in complex form, while non-coherent summation (see below) implies summation of the (squared) modulus (absolute magnitude) of complex numbers. Coherent summation is in theory more sensitive (because no information is discarded), but requires phase alignment to be maintained between the different signal components, i.e. on the different sub-carriers. However, if such alignment is not maintained, then non-coherent summation can be used. One common reason for losing phase alignment is due to ionospheric effects, which can introduce a frequency-dependent phase delay. Such ionospheric effects may therefore cause a loss of phase coherency across a wideband signal.

An alternative approach is set out in Equation 4 below:

$$\left|CCF_{NB}\left(\Delta\tau,\Delta f_d,t_k\right)\right| = \sqrt{\sum_{i=1}^{N_{sc}}\left|CCF_i\left(\Delta\tau,\Delta f_d,t_k\right)\right|^2} \quad \text{- (Equation 4)}$$

(Note that we could include $d_i^{Rx}(t_k)$ in Equation 4, as for Equation 3, however, because of the squared modulus, it would always multiply out to unity, and hence is redundant).

In the case of Equation 4, a non-coherent summation is performed, since the summation over the sub-carriers is of the squared modulus (rather than using a complex number summation). Note that in Figure 4, the output has the frequency width of one of the elementary correlation functions CCF_i. In effect, the non-coherent summation loses any

phase information across the different sub-carriers within a given epoch t_k, and so this reduces to a narrow-band system. Consequently, it is possible to relax the frequency search separation between two code hypotheses, and therefore the required sampling rate of the Doppler frequency space during code acquisition. The drawback of this approach (compared with the use of Equation 3) is that the non-coherent summation of the individual cross-correlation functions leads to larger and sometimes unacceptable sensitivity losses when N_{sc} becomes large.

The present approach seeks to reduce acquisition complexity by gathering together sub-carriers into sub-bands. This approach is suitable, for example, when the symbols transmitted on the different sub-carriers are the same or are known, so that it is possible to sum the elementary (complex) correlation functions coherently within each sub-band. This corresponds to the previous assumption that there is a single bit of data $d(t_k)$, e.g. navigation data, for the time interval from t_{k-1} to t_k, and this single bit of data then determines the values of $d_i(t_k)$ for this time interval according to a known mapping or arrangement. However, now we can potentially have a different data value, $d_{sb}(t_k)$, for each sub-band, where the value of $d_{sb}(t_k)$ for a given sub-band then determines the values of $d_i(t_k)$ for the sub-carriers within that particular sub-band according to a known mapping or arrangement. (This mapping may be the same for all sub-bands, or may vary from one sub-band to another).

The present approach utilises P sub-bands ($P \geq 2$), each sub-band comprising Q (adjacent) sub-carriers, ($Q \geq 2$), where the total number of sub-carriers is therefore given by $P*Q=N_{sc}$ (assuming all sub-carriers are transmitted). As shown in Equation 5, the Q correlation functions are summed coherently within each sub-band, while the P sub-bands are summed non-coherently, so that the detector output is given by:

$$\left|CCF_{SB}\left(\Delta\tau, \Delta f_d, t_k\right)\right| = \sqrt{\sum_{p=1}^{P}\left|\sum_{q=1}^{Q} d^{Rx}_{(p-1)\times Q+q}(t_k) \times CCF_{(p-1)\times Q+q}\left(\Delta\tau, \Delta f_d, t_k\right)\right|^2} \quad \text{(Equation 5)}$$

wherein:

- P is the number of sub-bands, processed non-coherently.
- Q is the number of sub-carriers per sub-band, processed coherently

Analogous to Equation 3, we again assume that $d(t_k)=1$ (or more precisely, that $d_{sb}(t_k)=1$), and then generate the test values of $d_i^{Rx}(t_k)$ (where $i=(p-1)\times Q+q$) using the known mapping for each sub-band as discussed above.

Note that if we set P=1 and hence Q= N_{sc}, we return to the wide-band processing of Equation 3 above; conversely, if we set Q=1 and hence P= N_{sc}, we return to the narrow-band processing of Equation 4 above. The processing of Equation 5 will be described herein as sub-band processing (to distinguish from that of Equations 3 and 4).

The expression of the elementary correlation function $CCF_{(p.1)\times Q+q}(\ldots)$ utilised in Equation 5 above can be derived from the former expression $CCF_i(\ldots)$ (Equation 2) to give the following:

$$CCF_{(p-1)\times Q+q}(\Delta\tau,\Delta f_d,t_k)=$$

$$\int_{t_k-1}^{t_k} s(t)\times(\exp(2\pi j(f_{(p-1)\times Q+q}+\Delta f_d)\times(t-\Delta\tau))\times p'(t-\Delta\tau))dt$$

(Equation 6)

where i from Equation 2 is now represented by $i=(p-1)\times Q+q$.

The above approach has been investigated using numerical simulations. As an example of these simulations, Figure 1 shows the power spectral density (PSD) of an orthogonal frequency division multiplex-code division multiple access signal (OFDM-CDMA) having a 1.023MHz chip rate. The multi-carrier signal has sub-carriers at [-20:2:20] *1.023MHz, except for the central frequency. In other words, in units of 1.023MHz, there are sub-carriers in the range from -20 to +20 with a spacing of 2, hence a total of N_{sc} = 20 (sub)carriers (since no carrier at the central frequency, i.e. at 0). The pulse, p(t), used for this illustration is a BPSK(1) signal (where the (1) indicates a frequency of 1*1.023MHz). In Figure 1 we can see that there are the 10 sub-carrier peaks on each side of the central frequency (shown as an offset of 0 MHz from the main carrier), and there is no peak at the central frequency.

Figure 2 shows the corresponding cross-correlation function for the wide-band acquisition, $CCF_{WB}(\Delta\tau,\Delta f_d)$, of the multi-carrier signal of Figure 1, i.e. calculated as per Equation 3 above. For these Figures, we assume that $\Delta f_d=0$, i.e. in effect the received signal

and the cross-correlated signal have an exact frequency match. Note that that Figure 2 includes both real and imaginary components (light grey and dark respectively) and the ordinate is normalised to a CCF of 1 at zero offset (delay). A zoom of the graph of Figure 2, centered on zero delay and using a logarithmic scale (still normalised to the CCF peak at zero delay), is provided in Figure 3. In Figure 3, the lighter grey represents the CCF value, while the darker (black) line indicates the delay at which the CCF has fallen 3dB with respect to the central peak at delay 0. In Figure 3 it can be seen that the 3dB fall-off from the central peak occurs at ±0.01 chip units from the central frequency. Accordingly, for the situation shown in Figures 1-3, if we want to use the full transmitted signal for the wide-band acquisition, then to avoid a sensitivity loss of more than 3dB, the minimum required sampling interval when searching Doppler frequency space is 1.023/50MHz. (=1 .023MHz*2*0.01) - in order to ensure a sample is taken from within the 3dB of the peak shown in Figure 3.

Alternatively, if the narrow-band processing of Equation 4 is applied to the same situation as illustrated in Figures 1-3, this produces the normalised cross-correlation function shown in Figure 4 (shown logarithmically, lighter line) for the narrow-band acquisition. As for Figure 3, Figure 4 also shows a darker (black) line that indicates the delay at which the CCF has fallen 3dB with respect to the central peak at delay 0. In Figure 4 it can be seen that the 3dB fall-off from the central peak occurs at ±0.3 chip units from the central frequency. In other words, as expected, for narrow-band processing, the CCF peak is spread out much more broadly. Consequently, the minimum required sampling interval when searching Doppler frequency space is 1.023/1.7MHz. (=1 .023MHz*2*0.3) in order ensure a sample is taken from within 3dB of the peak shown in Figure 4. This confirms, as expected, that the narrow-band processing of Equation 4 supports the use of a much coarser granularity of searching in frequency space than the wide-band processing of Equation 3.

Figure 5 is an analogous diagram to Figures 3 and 4, and shows a normalised cross-correlation function (logarithmic, lighter line) and also a darker (black) line that indicates the delay at which the CCF has fallen 3dB with respect to the central peak at delay 0. In particular, Figure 5 relates to the approach described herein (sub-band processing), based on Equation 5, in which multiple (Q) sub-carriers (narrow-band frequencies) are combined coherently within a sub-band, and multiple (P) sub-bands are then combined non-coherently.

For Figure 5, the following sub-bands were used (P=4, Q=5):

Sub-band 1: [-20,-18, -16, -14, -12] *1.023MHz centred at -16*1.023MHz

Sub-band 2: [-10, -8, -6,-4, -2] *1.023MHz centred at -6*1.023MHz

Sub-band 3: [2, 4, 6, 8, 10] *1.023MHz centred at 6*1.023MHz

Sub-band 4: [12, 14, 16, 18, 20] *1.023MHz centred at 16* l.023MHz

Note that each sub-band is formed from sub-carriers which are adjacent (consecutive or contiguous) in frequency. This has the effect of reducing the overall frequency spread within a given sub-band, which in turn increases the correlation width for acquisition purposes. In other words, using adjacent sub-carriers in a sub-band makes the sub-band more narrow-band, and hence supports a coarser granularity of Doppler frequency search.

In addition, because the sub-carriers in a given sub-band are added coherently, phase alignment must be maintained between all of the sub-carriers in the sub-band. As noted above, the main potential cause of loss of phase alignment is the effect of the ionosphere. This can be mitigated firstly by selecting consecutive sub-carriers, as above, to reduce the frequency spread of a sub-band, since this reduces any frequency-dependent ionospheric effect. In addition, having a symmetrical combination of sub-carriers about a central frequency can also help to mitigate ionospheric effects, in that any linear (first order) frequency-dependent ionospheric effect may cancel out above/below the central frequency. N.B. in the above example, Q=5, so there is a sub-carrier at the central frequency; however, the symmetrical arrangement may be preserved, even if there is no sub-carrier at the central frequency, e.g. if Q=4 , with sub-carriers at 14, 16, 18 and 20, which is symmetric about a (nominal) sub-carrier frequency of 17.

As shown in Figure 5, the 3dB fall-off from the central peak occurs at ±0.042 chip units from the central frequency (it will be appreciated that this is intermediate the values shown in Figures 3 and 4). Accordingly, for the situation shown in Figures 5, to avoid having a correlation loss of more than 3dB, the minimum required sampling interval when searching Doppler frequency space is 1.023/12 MHz. (=1 .023MHz*2*0.042) in order ensure a sample is taken from within 3dB of the peak shown in Figure 5 (again it will be appreciated that this is intermediate the values shown in Figures 3 and 4)

Figure 6 shows a comparison of the simulated acquisition dwell time against the carrier-to-noise ratio (C/N_0, in dB Hz) of the received signal. For the simulation, a

probability of false alarm of 0.1% was adopted, and also a probability of detection of 90%. In other words, the lines plotted in Figure 6 show the dwell time at which 90% of the individual simulations successfully acquired the signal with a probability of false alarm no more than 0.1%. The darker (black) line in Figure 6 represents the use of 4-sub-bands for signal acquisition, i.e. as per Equation 5, while the lighter line in Figure 6 represents the use of just 1 sub-band for signal acquisition, i.e. wide-band acquisition, as per Equation 3.

The integration time for the simulations was fixed to 10ms. For a high carrier-to-noise ratio, the dwell time=0.01s (10ms) – i.e. in effect, the signal was acquired in a single integration time. For a lower carrier-to-noise ratio, multiple integration times were needed to acquire the signal, leading to longer dwell times. (The step-like nature of Figure 6 arises because the dwell time is necessarily an integral number of integration times).

As expected, the wide-band approach of Equation 3 outperforms the multiple sub-band approach described herein, in that the line for the latter is located above the line for the former (implying longer dwell times). Nevertheless, for $C/N_0 > 31.5$ dBHz, there is no difference between the wide-band and four sub-band examples (both acquire in a single integration time), while for C/N_0 between 25dBHz and 31dBHz, the loss due to the non-coherent integration is only around 2dB in C/N_0. Accordingly, the approach described herein allows the wide-band signal acquisition complexity to be decreased without incurring major power losses. Moreover, the approach is flexible, in that the complexity can be tuned by selecting the number of sub-bands for any given receiver (and potentially for any given set of circumstances encountered by a given receiver).

As mentioned above, for the present approach the spreading code is transmitted using multiple sub-carriers, such as in an orthogonal frequency division multiplex scheme (OFDM). Figure 7 illustrates an example of the OFDM implementation for $N_{sc} = 8 (=2^3)$ sub-carriers, in which the different sub-carriers (at different respective frequencies) are set out along the x-axis, and the y axis represents increasing time epochs. At each time epoch t_k, 8 symbols are modulated and represented with a white circle for the 0 binary value and a black circle for the 1 binary value. Note that in practice, the number of sub-carriers may be significantly greater than 8, e.g. 16, 32, 64, 128 or 256. Note also that for reasons of clarity, the pulse shape p(t) (see Equation 1) and the corresponding spectral occupancy are not represented in Figure 7.

Figure 8 shows a variation on the OFDM implementation of Figure 7, in which not all sub-carriers are utilised at each epoch. In effect, we can represent a sub-carrier with a signal as having a value of ±1 (according to the value of the binary signal), while a sub-carrier with no signal has a value of 0, and hence does not contribute to the cross-correlation function. For example, in Figure 8, sub-carrier f_2 is not used at all, sub-carrier f_6 is not used at epoch t_{k+1}, and sub-carrier f_7 is not used at epochs t_{k+1}, t_{k+2}. Such a varying allotment or allocation of the N_{sc} sub-carriers with time may be used, for example, if the data rate of the spreading code is below the overall data rate capacity of the OFDM implementation.

Figure 9 shows a variation on the OFDM implementation of Figure 7, in which at each time epoch t_k, sub-groups of neighbouring (adjacent in frequency space) sub-carriers are modulated with the same symbols. As shown in Figure 9 for example, there are groups of paired sub-carriers f_1 & f_2, f_3 & f_4, f_5 & f_6 and f_7 & f_8, and the two sub-carriers within each pair transmit the same symbol as each other (which may change from one time epoch to another time epoch, as shown in Figure 9).

It is recognized that constraining neighbouring sub-carriers to be modulated with the same symbol, such as shown in Figure 9, reduces the effective transmitted information rate, due to the redundancy of symbol allocation. However, the allotment of the N_{sc} sub-carriers with time as shown in Figure 9 may be used, for example, if the data rate of the spreading code is below the overall data rate capacity of the OFDM implementation. The redundancy may also provide enhanced protection against noise, although in practice the robustness against narrow-band interference and multipath may not be improved significantly due to the spectral contiguity of the shared allocations shown in Figure 9.

Figure 10 shows a variation on the OFDM implementation of Figure 7, in which, for a given sub-carrier, there is a periodicity in the modulated symbols, such that the symbols modulated at epochs separated by a given time spacing, T_{per}, always have the same value.

The approaches shown in Figures 8-10 can be combined as appropriate, for example, as shown in Figure 11, in which pairs of sub-carriers are both modulated with the same symbol (analogous to Figure 9), but only a subset of the pairs of sub-carriers are transmitted at any epoch (analogous to Figure 8). Other such combinations of approaches (or further approaches) will be apparent to the skilled person.

Overall, the OFDM implementation illustrated in Figure 7 may be adapted or modified as appropriate, including with the introduction of one or more constraints, such as for Figures 8 to 11. The constraints may be adopted for various reasons, for example, in relation to data transmission rate, robustness, etc. In general, the constrained sequences are transmitted episodically and periodically (cyclically) – and the overall spreading code pattern is itself transmitted cyclically. In all implementations, the receiver is aware of the spreading code sequence to be received, and how this is allocated across the set of sub-carriers.

Figure 12 illustrates an implementation in which same symbol is repeated over T = 4 symbol durations. This approach (or similar) can help to improve the acquisition performance of a receiver by increasing the signal-to-noise ratio within the acquisition detector (albeit at the cost of a lower transmission rate for the code as a whole). In particular, successive correlations can be aggregated together over a period T for which the symbols on any given sub-carrier remain the same – i.e. T=4 for the example of Figure 12. In this case, the aggregated cross-correlation function calculated at the detector output is given by:

$$\left|CCF_{SB}\left(\Delta\tau,\Delta f_d,t_k\right)\right| = \sqrt{\sum_{p=1}^{P}\left|\sum_{t_k^{p,q}=t_k-T}^{t_k}\left(\sum_{q=1}^{Q} d^{Rx}_{(p-1)\times Q+q}(t_k)\times CCF_{(p-1)\times Q+q}\left(\Delta\tau,\Delta f_d,t_k^{p,q}\right)\right)\right|^2}$$

(Equation 7)

The CCF of Equation 7 is similar to that of Equation 5, except that there are now three summations, firstly over the sub-carriers (Q) in a given sub-band, secondly over the period T, representing the time interval from t_{k-1} to t_{k+2}, during which the symbols on any given sub-carrier remain constant, and thirdly over all sub-bands (P). The first two summations are performed coherently (within the modulus sign), the final summation is performed non-coherently (outside the modulus sign).

Figure 13 shows a further variation in the allocation of symbols to sub-carriers, in which all the sub-carriers belonging to a given sub-band must transmit the same symbols, but (unlike for Figure 9), not all at the same time, but rather at different times t_k and t_{k+U}. In the particular example of Figure 13, Q=2 and P=4 (N_{sc}=8), and the symbols are allocated, at times t_k and t_{k+U}, such that $d^{p,q0}(t_k) = d^{p,q1}(t_{k+U})$, ∀p=[1:P] and U=3, in which q0 and q1 represent the first and second sub-carriers respectively in a given band. This constraint

imposed on the symbols $d^{p,q0}(t_k)$ and $d^{p,q1}(t_{k+U})$ allows the elementary correlation functions $CCF_{(p-1)\times Q+q0}(\Delta\tau,\Delta f_d,t_k)$ and $CCF_{(p-1)\times Q+q1}(\Delta\tau,\Delta f_d,t_{k+U})$ to be added coherently at times t_k and t_{k+U}.

The skilled person can readily generalise the approach of Figure 13, which (because of the time difference) can help to improve demodulation in the presence of interference and/or multipath, to other values of Q, P and U. (Note that if only one symbol is transmitted at each time t_k ($\forall$k), the OFDM implementation of Figure 13 in effect becomes a form of frequency hopping, with one symbol transmitted at a time at a given frequency).

Figures 7-13 can therefore be seen as representing a mapping of data to the sub-carriers, analogous to the mapping from $d(t_k)$ to $d_i(t_k)$ discussed above, which information is then used in the correlations of Equations 3 and 5. Note that some of the data mappings shown in Figures 7-13 extend not only multiple sub-carriers, but also over multiple time intervals (t_k, t_{k+1}, etc). In some cases, the correlations described herein (see for example Figure 5) may be adjusted to extend over (or otherwise combine) such multiple time intervals, thereby exploiting knowledge of the relevant data mappings.

In some cases, the wide-band signal being received may represent a pilot signal, which may contain a spreading code (for example), but without encoding any data bits representing, e.g., navigation data. We can consider such a pilot signal as having a fixed data value, i.e $d(t_k)=1$ for all time intervals k, and this fixed data value is also known to the receiver for signal acquisition purposes. Note that, if desired, a mapping pattern such as discussed above in relation to Figures 7-13 might still be used for representing the fixed data value on the different subcarriers.

Figure 14 is a simplified schematic block diagram of an example of a receiver for implementing the approach described herein. Note that some receiver components of less direct relevance to the approach described herein are omitted for clarity. The receiver includes an aerial and associated circuitry 210 for receiving an incoming transmission signal (referred to as the wide-band signal). This signal is then passed to a demodulator 220, which is responsible for extracting the received symbol sequence within each sub-carrier (referred to as the narrow-band signal). Note that this demodulation may reflect or utilise any constraints imposed on the symbol sequences for the multiple sub-carriers, such as described above in relation to Figures 8-13.

The narrow-band signals are now passed to the channel acquisition unit 230 where they are cross-correlated against test signals for example representing the spreading codes of GNSS satellites. These test signals may be stored in, or generated by, code supply unit 240.

In many receivers, there are multiple hardware correlators 231A, 231B, 231C, 231D for performing different cross-correlations in parallel. For example, Figure 14 shows the receiver comprising 4 correlators, however, other receivers may have more or fewer hardware correlators. The hardware correlators 231A, 231B, 231C, 231D each perform narrow-band correlation, e.g. cross-correlating a given sub-carrier against a received signal in accordance with Equation 2 above.

For acquisition, the correlators are used to search a space based primarily on the following three parameters: (i) spreading code (different codes from different satellites); (ii) frequency (based on the range of potential Doppler shifts); and (iii) phase/time (based on the range of potential code delay). The test signal is primarily determined by the given spreading code for a given satellite (as per the first parameter). The frequency of the test signal (or the received signal) can then be adjusted, e.g. by re-sampling, to perform the search through frequency space. The timing/delay of the test signal can then be adjusted by altering the relative position (timing) of the test signal and the received signal in the correlator.

For a given test signal (for a particular code, frequency, and code delay), the narrow-band correlations are then combined within each sub-band as described above. In particular, narrow-band correlations within a single sub-band are added coherently, and these results for the different sub-bands are then added non-coherently to produce the final correlation result. For a given spreading code (for a given satellite), i.e. for a fixed parameter (i) above, the outcome of summing the sub-band cross-correlations at time epoch t_k, can be represented as $\left|CCF_{SB}(\Delta\tau, \Delta f_d, t_k)\right|$, as for Equation 5 above, where Δf_d reflects the frequency search value (parameter (ii) above) and $\Delta\tau$ reflects the delay search value (parameter (iii) above).

The coherent addition of the correlations for sub-carriers within a sub-band, followed by the non-coherent addition of the sub-band correlations, may be performed in the receiver of Figure 14 by a digital signal processing (DSP) unit 235 included within the channel acquisition unit 230. The allocation of sub-carriers to sub-bands may be stored in the channel acquisition unit 230, for example, within memory (not shown in Figure 14) associated with the DSP unit. In some receivers, it may be possible to update this memory to provide a new

allocation of sub-carriers to sub-bands. In other receivers, the allocation of sub-carriers to sub-bands may be fixed at a hardware level so that it cannot be reconfigured.

Although the above discussion of Figure 14 has focussed on channel acquisition, in some cases the same approach (and hardware) may also be used subsequently for tracking an acquired channel. On the other hand, since the frequency of the channel is known after acquisition, at this point is may be appropriate to use the full wide-band signal for tracking (in effect, setting $Q=N_{sc}$ and $P=1$).

It will be appreciated that Figure 14 is provided by way of example only, and the skilled person will be aware of many other possible implementations. For example, one potential hardware implementation is based on the use of a FPGA (Field programmable Gate Array).

Figure 15 is a flowchart illustrating an example of a method for implementing the approach described herein, as performed by a receiver. The method includes receiving a wide-band signal comprising N narrow-band signals (operation 310), for example, wide-band GNSS signal. The wide-band signal uses frequency division multiplexing to accommodate the N narrow-band signals on respective sub-carriers at different frequencies within the wide-band signal. For each of the N narrow-band signals, the received narrow-band signal may be cross-correlated to produce a sub-carrier cross-correlation function (operation 320).

At the receiver, the wide-band signal is considered to represent P sub-bands, where $P \geq 2$, each sub-band comprises one or more sub-carriers, and each sub-carrier accommodates a respective one of the N narrow-band signals. The method further comprises, for each sub-band, coherently summing the one or more sub-carrier cross-correlation correlation functions for that sub-band to create a sub-band cross-correlation function (operation 330). The sub-band cross-correlation functions of all of the P sub-bands are now summed non-coherently (operation 340) to produce a wide-band cross-correlation function for the wide-band signal.

In this approach, the wide-band signal can be regarded as a sum of multiple elementary narrow-band signals, all offset with respect to a central carrier frequency. Each narrow-band signal is, for example, down-converted to the carrier and correlated with a replica matched to the corresponding narrow-band signal. Such a solution is able to generate a cross-correlation function which is wider (in frequency space) than the cross-correlation function for the whole wide-band signal, therefore enabling a relaxation (reduction in) the

number of code hypotheses to be searched. In particular, the resulting cross-correlation function produced by the method described herein is as wide (in frequency space) as the cross-correlation function from one of the elementary narrow-band signals.

The above approach may be used, for example, for OFDM communications and/or for position determination in GNSS systems. In the latter case, each narrow-band signal may be modulated by the spreading code for a given satellite. In signal acquisition, the narrow-band signal can be correlated against a spreading code for a (trial) satellite. If the trial satellite is the same as the given satellite, the correlation will then produce a peak for each narrow-band signal, thereby confirming that the given satellite has been acquired. Conversely, if the trial satellite is not the same as the given satellite, the mismatch in spreading codes will lead to a correlation result of (approximately) zero, and hence it will be apparent that the trial satellite has not been acquired.

Accordingly, the approach described herein has the effect of widening the correlation function, thereby decreasing the acquisition complexity for a wide-band signal (such as by reducing the number of code and Doppler mis-alignment hypotheses required). In addition, the approach described herein also helps to reduce the power consumption of the receiver, as acquisition usually represents a high peak of energy consumption, since energy consumption increases with computational complexity.

For a wide-band signal, N is generally in the range 10-400, more typically 40-200 (although other values are possible). The difference in correlation width between the wide-band signal and the narrow-band signals is therefore substantial.

In some implementations, each sub-band comprises the same number of sub-bands, Q, where $Q \geq 2$; for example, Q may lie in the range 2-100, more typically 4-50, more typically 8-25, and P may lie in the range 2-100, more typically 4-50, more typically 8-25. For a fixed N (=P*Q), having a larger value of Q will provide greater search sensitivity, because more sub-carriers are combined coherently. In some cases at least, a practical upper value on Q may be imposed by loss of phase coherence between different sub-carriers, e.g. due to atmospheric or ionospheric phase-dependent propagation delays.

Note that the values of P and Q are selected by the receiver, rather than being inherent to the transmitted signal. Rather, the transmitted signal comprises a wide-band signal formed from N narrow-band components. It is up to a given receiver how these N narrow-band

components are split (if at all) into sub-bands. Different receivers may split with different values of P and Q according to the design priorities of a given receiver (sensitivity, cost, acquisition time, etc). In some receivers at least, the number of sub-bands (i.e. the value of P) and/or the allocation of the sub-carriers to the sub-bands, may be (re)configurable in the receiver itself, whether through user input, or potentially in response to operating conditions (strength and stability of received signal, etc).

Typically the sub-carriers in a given sub-band are contiguous in frequency (i.e. sequential if the sub-carriers are ordered by frequency). Consequently, the sub-bands correspond to (non-overlapping) respective frequency bands. Contiguous sub-carriers are more likely to maintain phase alignment against frequency-dependent propagation effects.

In some implementations, the wide-band signal transmits a symbol sequence, and the frequency division multiplexing imposes one or more constraints on the how the symbols are allocated to the sub-carriers. For example, the one or more constraints comprises at least one of the following: (i) for each sub-band, identical symbols are allocated to the one or more sub-carriers that sub-band (as per Figure 9); (ii) for any given sub-carrier, the symbols are transmitted with a periodicity in time (as per Figure 11); (iii) the sub-carriers are paired, such that a symbol transmitted on a first sub-carrier in a pair is subsequently transmitted on the other sub-carrier in the pair (as per Figure 13). The skilled person will be aware of other possible constraints to impose on the symbol allocations, and the pros and cons thereof.

The above processing has generally described an implementation in which there is a single carrier that supports multiple sub-carriers. In other implementations, there may be multiple separate, narrow-band carriers (without there being any overall single carrier), in which case each narrow-band carrier could be regarded as a separate sub-carrier (although this may possibly provide an additional potential source for loss of phase alignment). More generally, the approach described herein can be used for any wide-band signal with multiple (sub)carriers and for any combination of the different OFDM signal options; it is also independent of the pulse shape characteristics, p(t)).

The processing described herein is generally performed by a receiver. The functionality of the receiver is generally controlled by the combination of the software and hardware of the receiver. The software comprises one or more programs, comprising machine readable instructions, that execute on the hardware of the receiver (e.g. on one or more processors within the receiver) to cause the receiver to implement the desired

functionality. In some cases, at least some of the software may be executed on a general purpose processor, such as digital signal processor. In some cases, the software may be stored in the receiver, e.g. in flash memory, a disk drive, or other storage device. The software may be loaded into the receiver by any suitable mechanism, such as by wireless transmission, or insertion of a physical storage medium into the receiver. In some cases, at least some or all of the functionality may be implemented directly in hardware.

In conclusion, the skilled person will be aware of various modifications that can be made to the above examples to reflect the particular circumstances of any given implementation. Moreover, the skilled person will be aware that features from different examples can be mixed as appropriate in any particular implementation, without limitation to the particular combinations described in the above examples. Accordingly, the scope of the present invention is defined by the appended claims and their equivalents.

Claims

1. A method performed by a receiver, the method comprising:

(a) receiving a wide-band signal comprising N narrow-band signals, the wide-band signal using frequency division multiplexing to accommodate the N narrow-band signals on respective sub-carriers at different frequencies within the wide-band signal;

(b) dividing the wide-band signal into P sub-bands, where $P \geq 2$, each sub-band comprising one or more sub-carriers, each sub-carrier accommodating a respective one of the N narrow-band signals, and at least one sub-band comprising two or more sub-carriers;

(c) for each of the N narrow-band signals, correlating the received narrow-band signal to produce a sub-carrier cross-correlation function;

(d) for each sub-band, coherently summing the one or more sub-carrier cross-correlation functions for that sub-band to create a sub-band cross-correlation function; and

(e) summing non-coherently the sub-band cross-correlation functions of all of the P sub-bands to produce a cross-correlation function for the wide-band signal.

2. The method of claim 1, wherein each sub-band comprises the same number of sub-bands, Q, where $Q \geq 2$.

3. The method of claim 2, wherein each sub-band comprises the same number of sub-bands, Q, where Q is in the range 2-100, more typically 4-50, more typically 8-25.

4. The method of any preceding claim, wherein P is in the range 2-100, more typically 4-50, more typically 8-25.

5. The method of any preceding claim, wherein N is in the range 10-400, more typically 40-200.

6. The method of any preceding claim, further comprising configuring the value of P and/or the allocation of the sub-carriers to the sub-bands.

7. The method of any preceding claim, wherein, for each sub-band containing two or more sub-carriers, said two or more sub-carriers are contiguous in frequency.

8. The method of any preceding claim, wherein, for each sub-band containing two or more sub-carriers, said two or more sub-carriers are contained within a sufficiently narrow frequency range to maintain phase alignment between the two or more sub-carriers.

9. The method of claim 8, wherein maintaining phase alignment between the two or more sub-carriers for a sub-band includes having a symmetric arrangement of the two or more sub-carriers for the sub-band about a central frequency of the sub-band.

10. The method of claim 9, wherein the symmetric arrangement compensates for first order atmospheric and ionospheric frequency-dependent phase disparity.

11. The method of any preceding claim, wherein the output of steps (c)-(e) at time epoch t_k is: $\left|CCF_{SB}\left(\Delta\tau,\Delta f_d,t_k\right)\right| = \sqrt{\sum_{p=1}^{P}\left|\sum_{q=1}^{Q} d^{Rx}_{(p-1)\times Q+q}(t_k)\times CCF_{(p-1)\times Q+q}\left(\Delta\tau,\Delta f_d,t_k\right)\right|^2}$

(Equation 5)

wherein: P is the number of sub-bands, processed non-coherently; Q is the number of sub-carriers per sub-band, processed coherently; $\Delta\tau$ represents the delay misalignment error between the received signal and the test signal; Δf_d the frequency misalignment error between the received signal and the test signal; and d_i is a data symbol on a sub-carrier i.

12. The method of any preceding claim, wherein the wide-band signal transmits a symbol sequence, and the frequency division multiplexing imposes one or more constraints on the how the symbols are allocated to the sub-carriers.

13. The method of claim 12, wherein the one or more constraints comprises at least one of the following constraints:

(i) for each sub-band, identical symbols are allocated to the one or more sub-carriers that sub-band;

(ii) for any given sub-carrier, the symbols are transmitted with a periodicity in time.

(iii) the sub-carriers are paired, such that a symbol transmitted on a first sub-carrier in a pair is subsequently transmitted on the other sub-carrier in the pair.

14. The method of any preceding claim, wherein the frequency division multiplexing comprises orthogonal frequency division multiplexing.

15. The method of any preceding claim, wherein the sub-carriers are provided as respective, separate, narrow-band carriers.

16. The method of any preceding claim, wherein the wide-band signal comprises a code for a code-division multiple access system.

17. The method of any preceding claim, wherein the wide-band signal comprises a wide-band global navigation satellite system (GNSS) signal comprising a spreading code for use in determining the location of the receiver.

18. The method of claim 17, wherein steps (c)-(e) are performed as part of acquiring the spreading code at the receiver.

19. The method of claim 18, wherein step (c) includes correlating the received narrow-band signals against one or more known spreading codes for the global navigation satellite system.

20. The method of claim 18 or 19, wherein the acquiring includes providing multiple test signals at different respective frequencies for searching for the spreading code through Doppler space.

21. A receiver configured to:

(a) receive a wide-band signal comprising N narrow-band signals, the wide-band signal using frequency division multiplexing to accommodate the N narrow-band signals on respective sub-carriers at different frequencies within the wide-band signal;

(b) divide the wide-band signal into P sub-bands, where $P \geq 2$, each sub-band comprising one or more sub-carriers, each sub-carrier accommodating a respective one of the N narrow-band signals, and at least one sub-band comprising two or more sub-carriers;

(c) for each of the N narrow-band signals, correlate the received narrow-band signal with a test signal to produce a sub-carrier cross-correlation function;

(d) for each sub-band, coherently sum the one or more sub-carrier cross-correlation correlation functions for that sub-band to create a sub-band cross-correlation function; and

(e) sum non-coherently the sub-band cross-correlation functions of all of the P sub-bands to produce a cross-correlation function for the wide-band signal.

22. The receiver of claim 21, wherein the wide-band signal comprises a wide-band global navigation satellite system (GNSS) signal comprising a spreading code, and wherein the receiver is configured to use the received spreading code for determining the location of the receiver.

23. The receiver of claim 21 or 22, wherein the receiver is configured to support a re-allocation of sub-carriers to sub-bands.

24. The receiver of claim 23, wherein the receiver is configured to support a change in the number of sub-bands.

25. The receiver of claim 23 or 24, receiver is configured to sense reception conditions for the wide-band signal, and to re-allocate the sub-carriers to sub-bands and/or the change the number of sub-bands based on the sensed conditions.

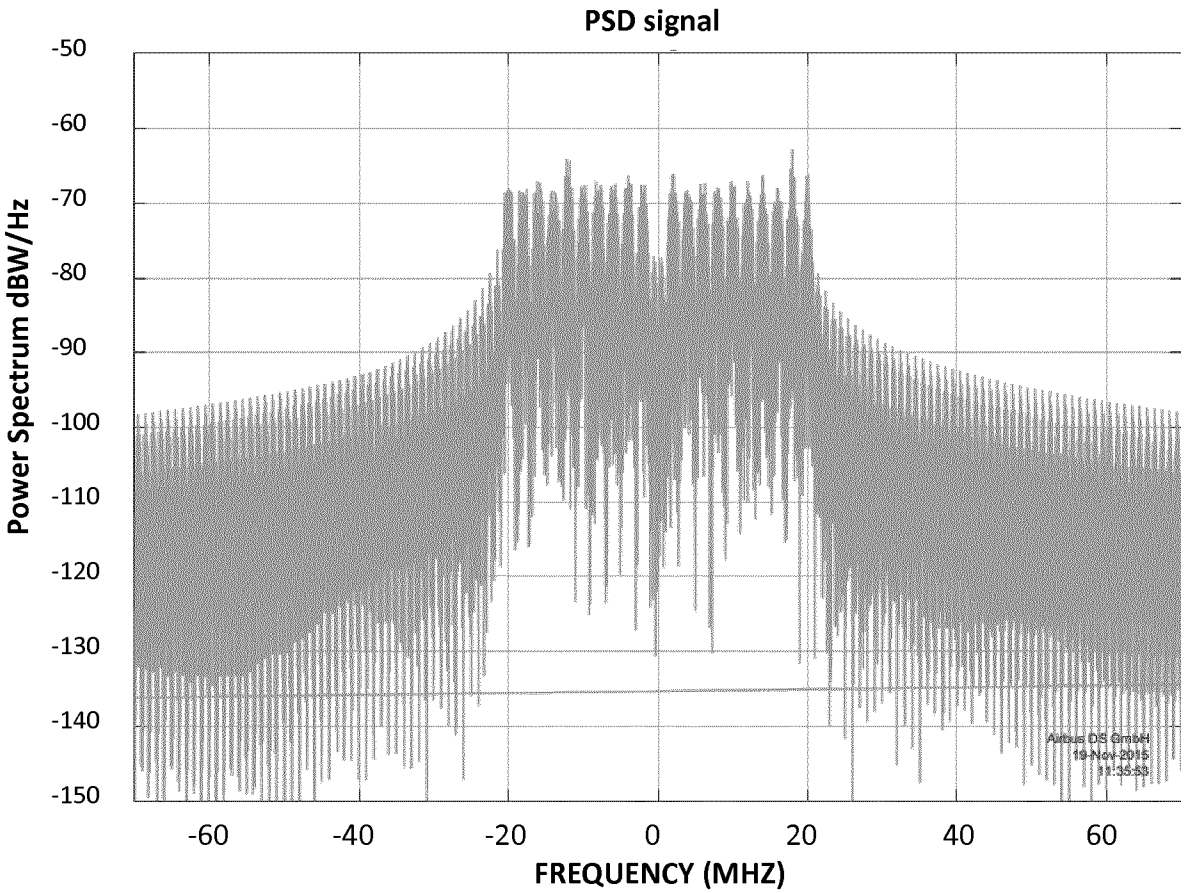

PSD signal
Power Spectrum dBW/Hz
-50
-60
-70
-80
-90
-100
-110
-120
-130
-140
-150
-60
-40
-20
0
20
40
60
FREQUENCY (MHZ)
Airbus DS GmbH
19-Nov-2015
11:35:53

Figure 1

A = Real CCF BPSK(1)
B= Imag CCF (BPSK(1)

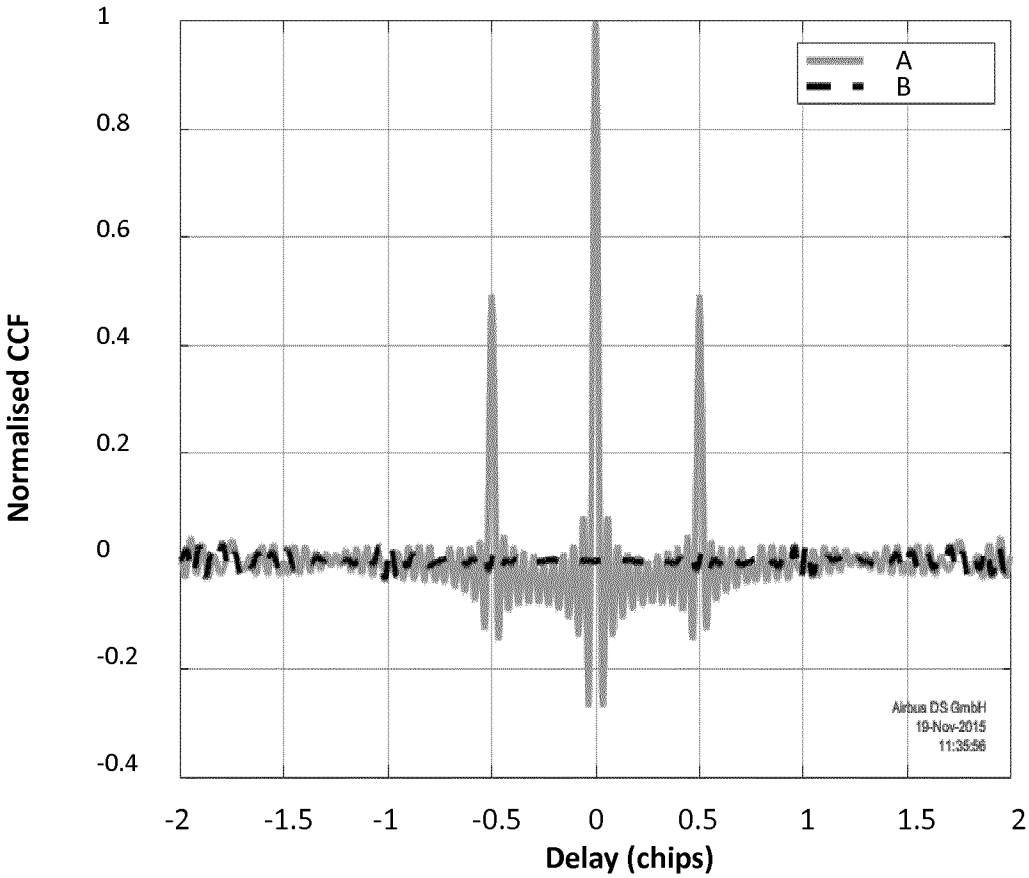


Figure 2

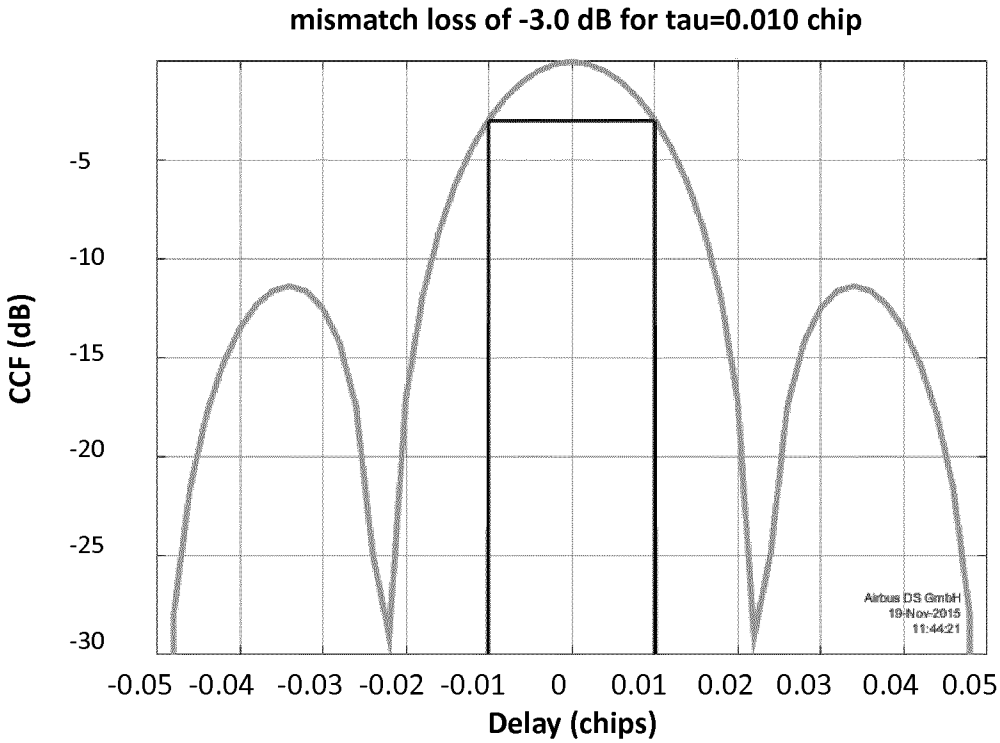

mismatch loss of -3.0 dB for tau=0.010 chip
CCF (dB)
-5
-10
-15
-20
-25
-30
-0.05 -0.04 -0.03 -0.02 -0.01 0 0.01 0.02 0.03 0.04 0.05
Delay (chips)
Airbus DS GmbH
19-Nov-2015
11:44:21

Figure 3

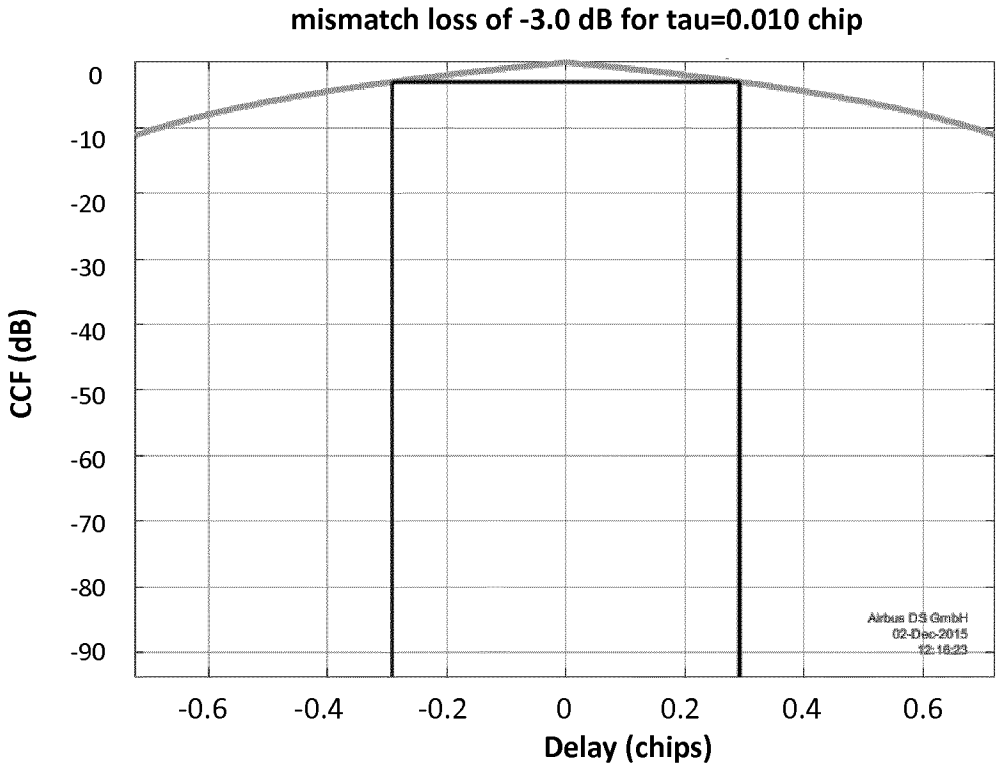

mismatch loss of -3.0 dB for tau=0.010 chip
CCF (dB)
0
-10
-20
-30
-40
-50
-60
-70
-80
-90
-0.6
-0.4
-0.2
0
0.2
0.4
0.6
Delay (chips)
Airbus DS GmbH
02-Dec-2015
12:16:23

Figure 4

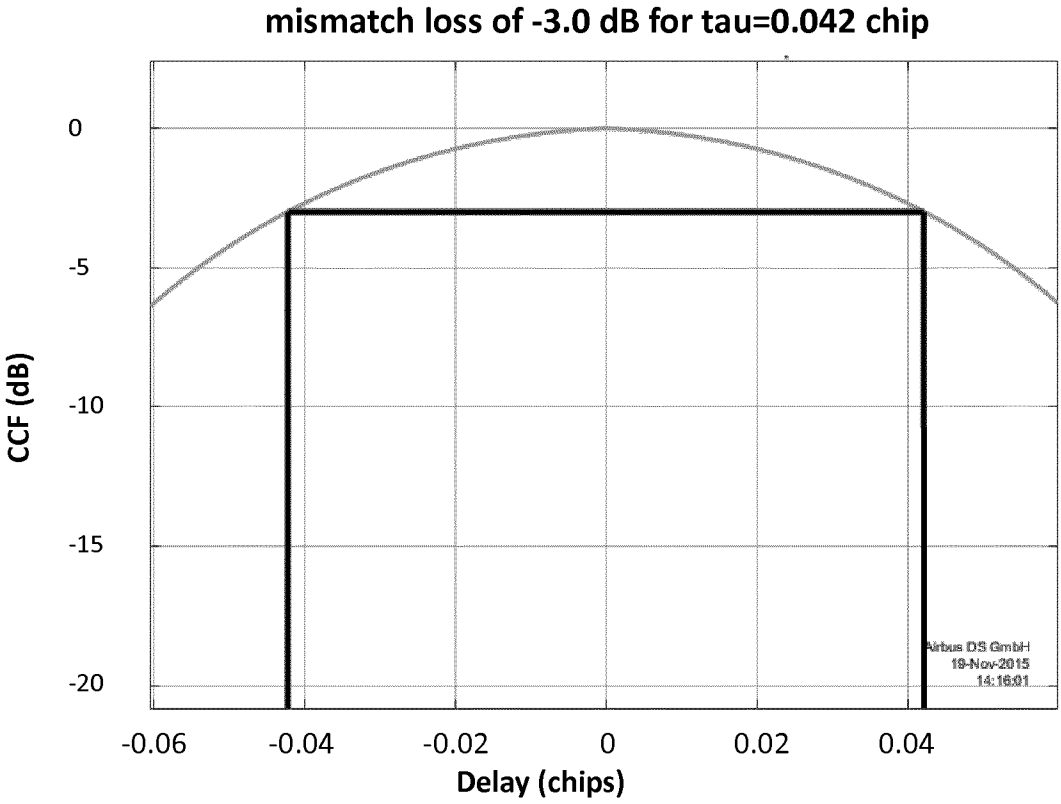

mismatch loss of -3.0 dB for tau=0.042 chip
0
-5
-10
-15
-20
CCF (dB)
-0.06
-0.04
-0.02
0
0.02
0.04
Delay (chips)
Airbus DS GmbH
19-Nov-2015
14:16:01

Figure 5

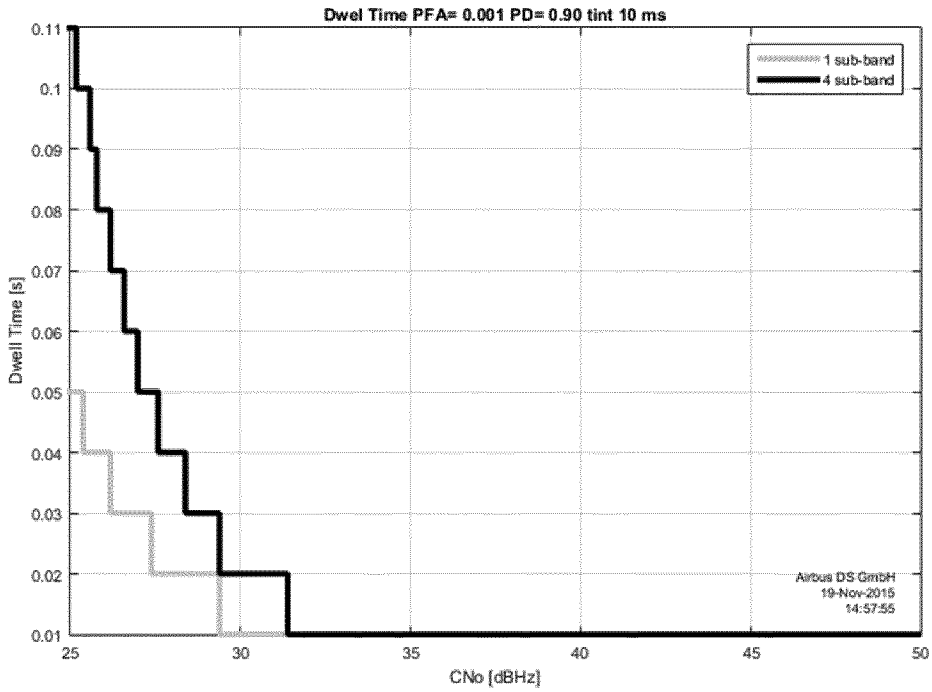

Dwel Time PFA= 0.001 PD= 0.90 tint 10 ms
1 sub-band
4 sub-band
Dwell Time [s]
CNo [dBHz]
Airbus DS GmbH
19-Nov-2015
14:57:55

Figure 6

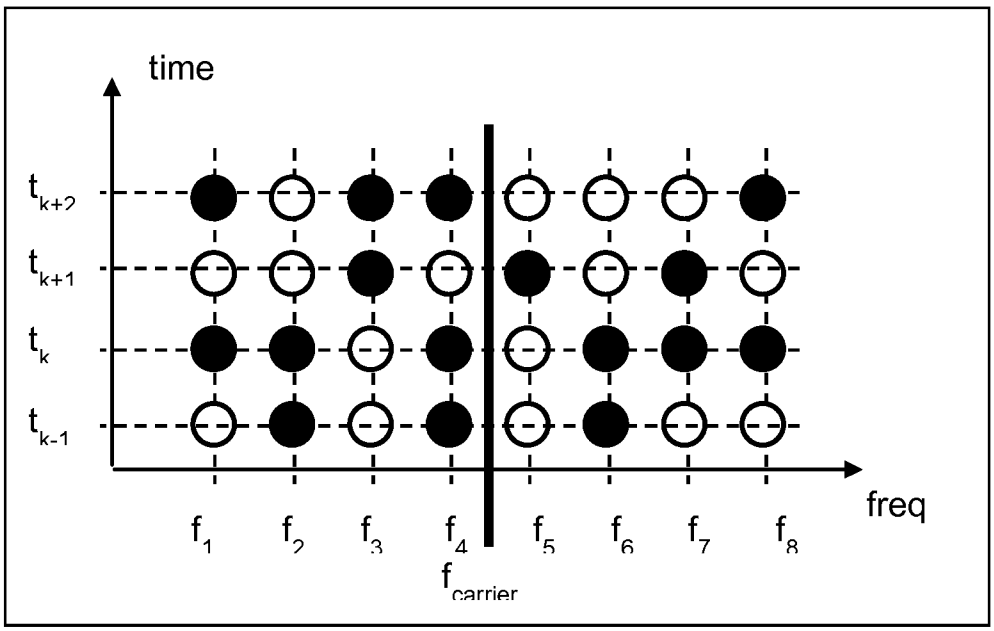


Figure 7

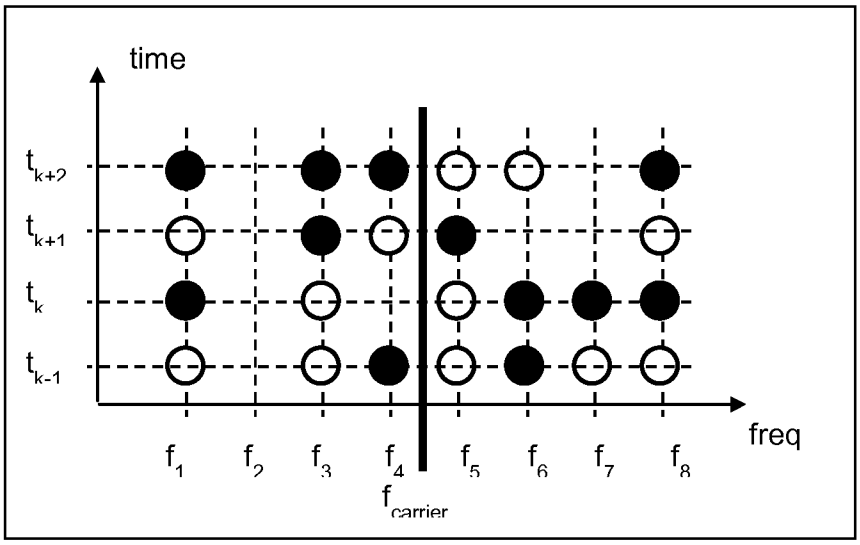


Figure 8

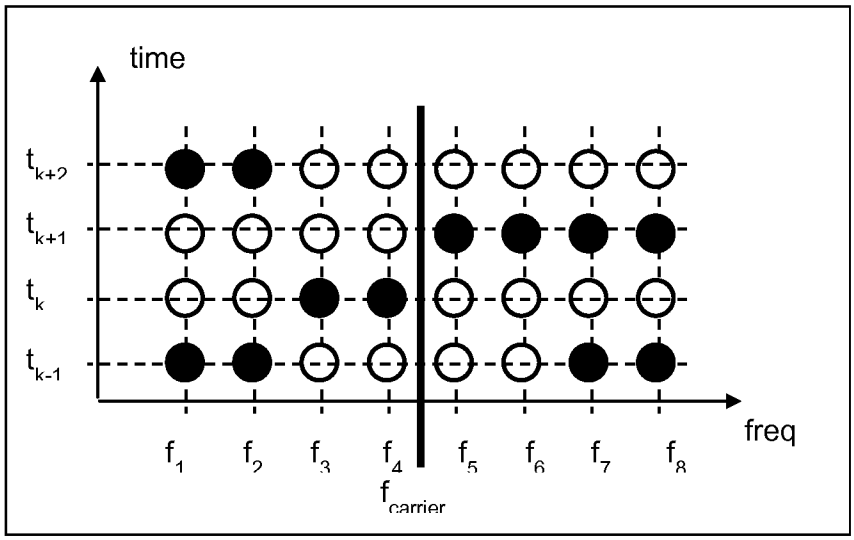


Figure 9

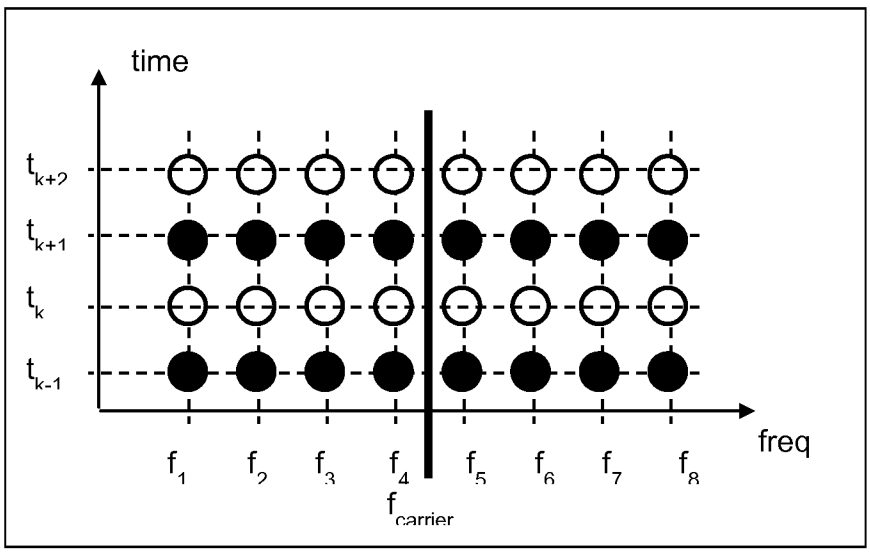


Figure 10

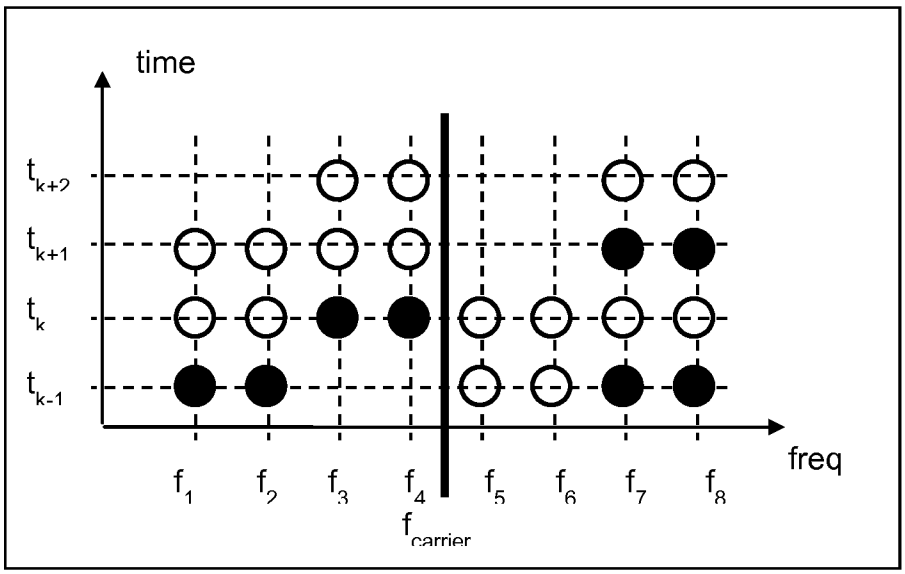


Figure 11

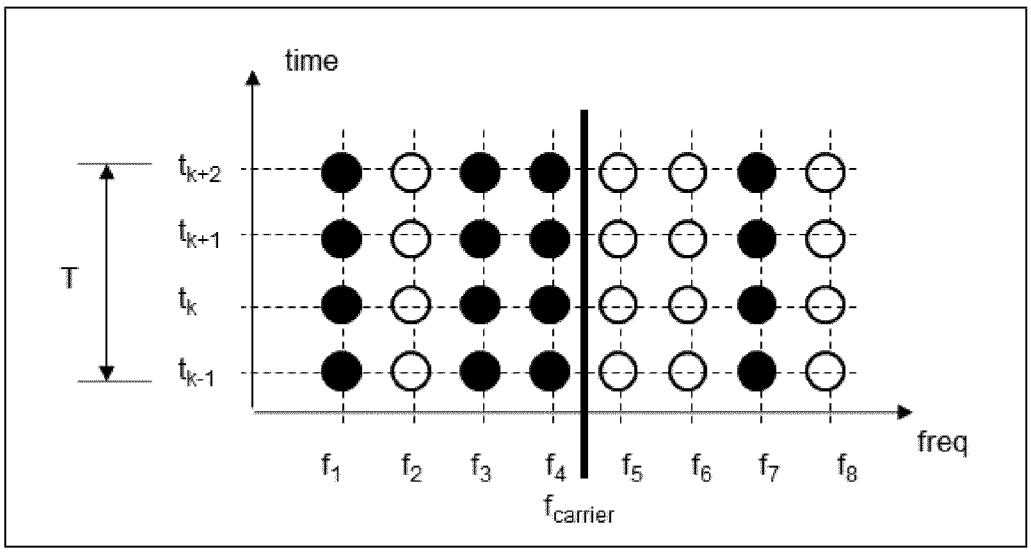


Figure 12

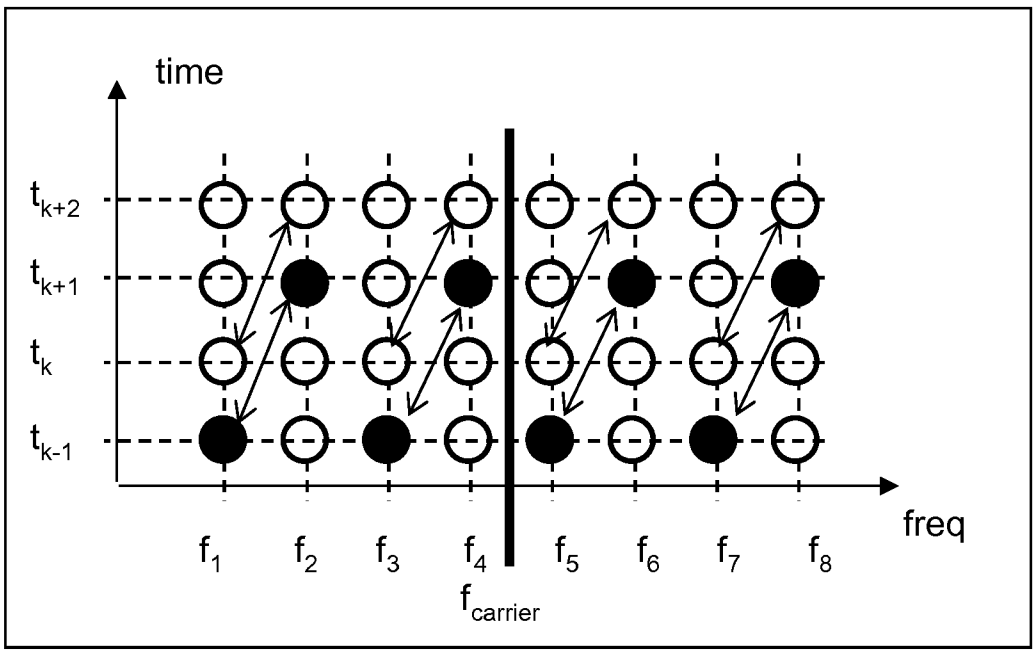


Figure 13

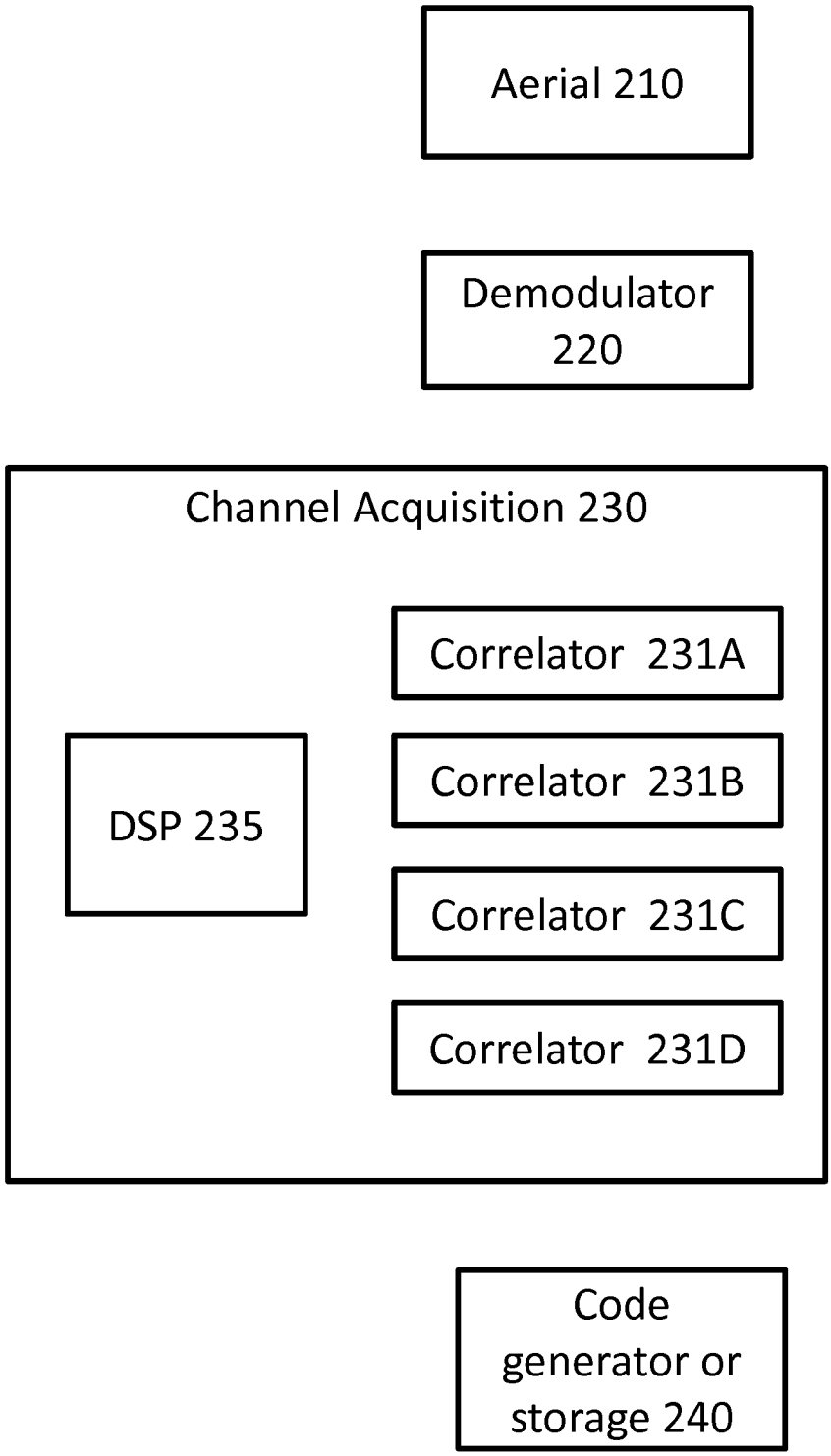

Aerial 210
Demodulator 220
Channel Acquisition 230
Correlator 231A
Correlator 231B
Correlator 231C
Correlator 231D
DSP 235
Code generator or storage 240

Figure 14

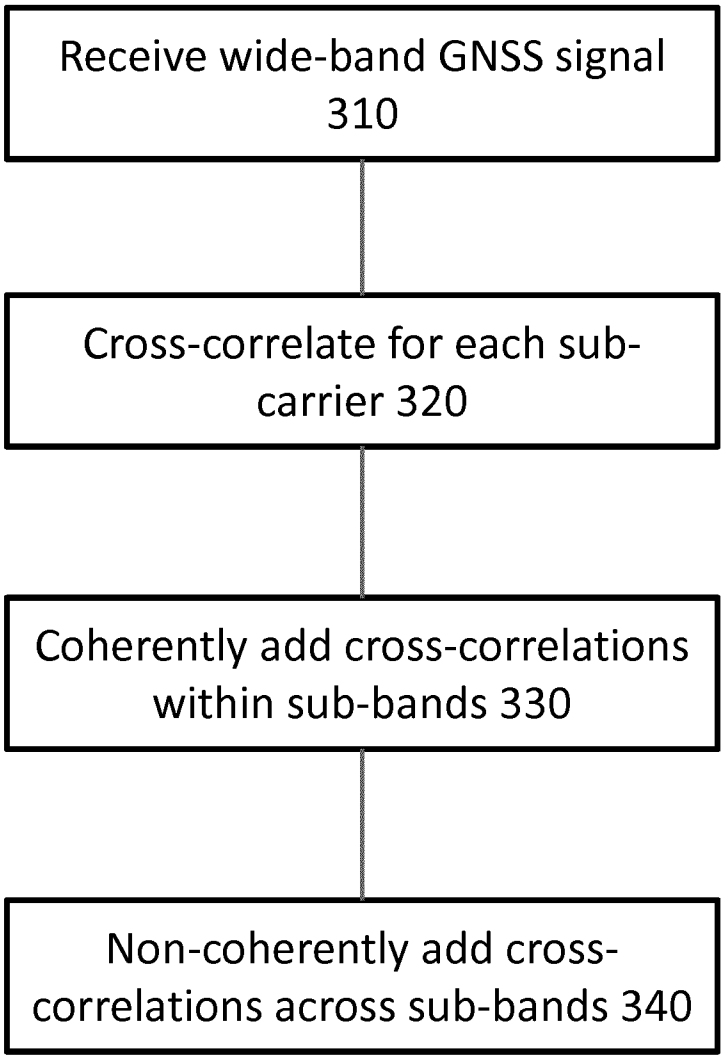

Receive wide-band GNSS signal 310
Cross-correlate for each sub-carrier 320
Coherently add cross-correlations within sub-bands 330
Non-coherently add cross-correlations across sub-bands 340

Figure 15

INTERNATIONAL SEARCH REPORT

International application No
PCT/EP2017/069235

A. CLASSIFICATION OF SUBJECT MATTER
INV. G01S19/30 H04L27/26 H04W56/00 H04J11/00
ADD. G01S19/02

According to International Patent Classification (IPC) or to both national classification and IPC

B. FIELDS SEARCHED

Minimum documentation searched (classification system followed by classification symbols)
G01S H04L H04W H04J

Documentation searched other than minimum documentation to the extent that such documents are included in the fields searched

Electronic data base consulted during the international search (name of data base and, where practicable, search terms used)

EPO-Internal, WPI Data

C. DOCUMENTS CONSIDERED TO BE RELEVANT

Category*	Citation of document, with indication, where appropriate, of the relevant passages	Relevant to claim No.
X	EP 3 057 252 A1 (FREESCALE SEMICONDUCTOR INC [US]) 17 August 2016 (2016-08-17) paragraph [0007] paragraph [0019] paragraph [0029] - paragraph [0103] -----	1-25
X	GARCIA-PENA A ET AL: "FMT Signal Options and Associated Receiver Architectures for GNSS", NAVIGATION: JOURNAL OF THE INSTITUTE OF NAVIGATION, 26 April 2012 (2012-04-26), pages 898-912, XP056003862, ISSN: 0028-1522, DOI: 10.1109/PLANS.2012.6236833 page 898 - page 905 -----	1-25

☐ Further documents are listed in the continuation of Box C.

☒ See patent family annex.

* Special categories of cited documents :

"A" document defining the general state of the art which is not considered to be of particular relevance

"E" earlier application or patent but published on or after the international filing date

"L" document which may throw doubts on priority claim(s) or which is cited to establish the publication date of another citation or other special reason (as specified)

"O" document referring to an oral disclosure, use, exhibition or other means

"P" document published prior to the international filing date but later than the priority date claimed

"T" later document published after the international filing date or priority date and not in conflict with the application but cited to understand the principle or theory underlying the invention

"X" document of particular relevance; the claimed invention cannot be considered novel or cannot be considered to involve an inventive step when the document is taken alone

"Y" document of particular relevance; the claimed invention cannot be considered to involve an inventive step when the document is combined with one or more other such documents, such combination being obvious to a person skilled in the art

"&" document member of the same patent family

Date of the actual completion of the international search	Date of mailing of the international search report
10 April 2018	18/04/2018

Name and mailing address of the ISA/	Authorized officer
European Patent Office, P.B. 5818 Patentlaan 2 NL - 2280 HV Rijswijk Tel. (+31-70) 340-2040, Fax: (+31-70) 340-3016	Haugg, Sabine

INTERNATIONAL SEARCH REPORT

Information on patent family members

International application No
PCT/EP2017/069235

Patent document cited in search report	Publication date	Patent family member(s)	Publication date
EP 3057252 A1	17-08-2016	CN 105897641 A	24-08-2016
		EP 3057252 A1	17-08-2016
		US 2016242103 A1	18-08-2016